



Phonon Spectrum of Distorted Graphene with Stone-Wales Dislocations at Tersoff and Airebo Potential

P. P. Jadhav,^{1,2} and R.S. Vhatkar^{2,*}

¹Department of Physics, Balwant College, Vita, 415311, Maharashtra, India.

²Department of Physics, Shivaji University, Kolhapur, 416004, Maharashtra, India.

*E-mail: drvhatkar@gmail.com

ABSTRACT

Phonon density of states of pristine graphene and graphene with Stone-Wales dislocations was investigated using nonequilibrium molecular dynamics simulations using SiC Tersoff potential, SiC Ge Tersoff potential and AIREBO potential. By the computation of phonon density of states, the performance of these potentials is evaluated. Temperature distribution of pristine graphene and graphene with Stone-Thower-Wales Dislocation is found to be conserved at 300K. In this nonequilibrium molecular dynamics simulation (NEMD), Heat flux is calculated for pristine graphene and graphene with Stone-Wales dislocation for Tersoff Potential and AIREBO potential. Radial density profile is evaluated to check structural changes in pristine graphene and graphene with Stone-Wales Dislocation at Tersoff and AIREBO potential. Due to phonon density of states (PDOS) of graphene with Stone-Wales Dislocation phonon scattering enhances. At high frequency domain, softening of phonon modes is observed which indicates reduction in thermal conductivity. Thus, reduction in thermal conductivity of graphene with Stone-Wales Dislocation as compared to the thermal conductivity of pristine graphene.

Keyword: Pristine Graphene, Stone-Thower-Wales Dislocations, Tersoff Potential, AIREBO Potential, Phonon Density of States (PDOS), Molecular Dynamics Simulations.

Received 17.02.2022

Revised 18.03.2022

Accepted 20.04.2022

INTRODUCTION

Graphene is perfect test bed to provide correlation between thermal transport property and graphene with defects [1]. Graphene is a single layer of graphite having lattice structure of honeycomb. It has series of applications since its discovery. [2] In two dimensional materials, to support perfect test bed, graphene is important. [3] Nonequilibrium molecular dynamics simulations (NEMD) method that is utilized to obtain phonon density of states of pristine graphene nanosheet and graphene with Stone-Wales dislocation. In many materials, phonons are of utmost important. Most of the properties of the materials are directly or indirectly derived from phonon density of states (PDOS) [4]. Phonon transport leads to heat dissipation, energy storage, saving, thermoelectric energy conversion, shielding [5]. Nanodevices have smaller size than phonon mean free path in such case, phonon travels without dissipation of energy and scattering and becomes ballistic. Power spectrum is good estimate for the qualitative and quantitative analysis purpose. [6]. Phonon is a quantized mode of lattice vibrations; Phonons have an important role in material's thermal and electrical conductivities. The properties of long wavelength phonon's give rise to sound in materials so the name phonon.

The phonon density of states or phonon spectra is computed from the velocity autocorrelation function (VACF) by the use of Fourier transform.

$$P(\omega) = \frac{1}{\sqrt{2\pi}} \int e^{i\omega t} \left[\sum_{j=1}^{N_j} v_j(t) v_j(0) \right] dt \quad (1)$$

Where $v_j(t)$ and $v_j(0)$ is the velocity of j th particle at time t and 0 respectively, $P(\omega)$ is phonon spectrum function, ω is vibrational wave number [2,7].

The two-dimensional structure of the graphene is reflected by the phonon density of states. Phonon density of states is used to reveal the mechanism of conduction of heat. [8] Tersoff potential and AIREBO

potential is able to reproduce power spectra or phonon density of states in pristine graphene and graphene with Stone-Wales dislocations. Between pristine and distorted graphene, knowledge of the mechanism of heat transport using phonon spectrum is very limited. Phonon spectrum helps to understand thermal conductivity of distorted graphene. The findings of this work are useful to reveal the phononic mechanism through defect engineering. This work is helpful to engineer low thermal conductivity nanodevices.

MATERIAL AND METHODS

In this work, atomistic molecular dynamics simulation is implemented to calculate power spectra of pristine graphene and graphene with Stone-Wales dislocations at various potentials such as Tersoff potential and AIREBO potential. The armchair graphene nanosheet with 200 atoms and distorted graphene with Stone-Wales dislocation as shown in figure 1a) and 1b) are generated by using software OVITO[9].

Stone Wales Dislocations: Stone-Wales Dislocations are also known as Stone-Thrower Wales Dislocations or heptagon-pentagon(7-5), pentagon-heptagon(5-7), or (5-7-7-5) dislocations[10][11] and can be generated by rotating C-C bond 90 degrees in which four carbon hexagons turn into two heptagons and two pentagons. Dislocations are spread over graphene nanosheet but periodicity of the graphene nanosheet remains constant. Stone-Wales Dislocations [11] does not involve any removal or addition of atoms.

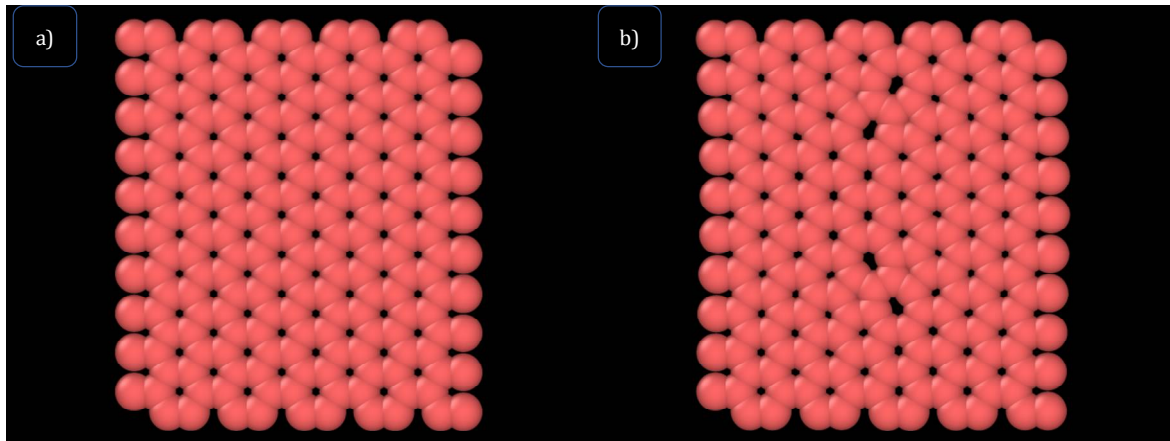


Figure1: a) Pristine graphene b) Distorted graphene with Stone-Wales Dislocation

The graphene nanosheet with dimension (24.5951 Å X 21.3000 Å X 5 Å) having armchair direction with 200 atoms is simulated in canonical ensemble (NVT) also known as constant volume and constant temperature ensemble by the time integration of Noose-Hoover thermostat at a temperature of 300K with time step 2 femtosecond. Simulations are run in the in-house code of atomic scale modeling at 10,000 time steps.[12]

Potentials used:

- 1) Tersoff Potential:** In Tersoff potential[13], energy is sum of pair like interactions. The Tersoff Potential is having original functional forms [14] and parameterization[15]. The site energy E is given by

$$E = \sum_i E_i = \frac{1}{2} \sum_{i \neq j} V_{ij} \quad (2)$$

Where V_{ij} is bond energy

$$V_{ij} = f_c(r_{ij}) [a_{ij} f_R(r_{ij}) + b_{ij} f_A(r_{ij})] \quad (3)$$

Here f_R is repulsive pair potential function and f_A is attractive pair potential function, f_c is cut off function[16]

$$f_R(r) = A \exp(-\lambda_1 r) \quad (4)$$

$$f_A(r) = -B \exp(-\lambda_2 r) \quad (5)$$

- 2) AIREBO Potential:** The modified form of Brenner Potential described by Stuart et.al in 2000 is AIREBO Potential. So as to improve the accuracy of hydrocarbon and diamond like

structures.[15]Improved form of REBO is AIREBO potential known as adaptive intermolecular reactive empirical bond order potential[17].It includes a component of non-bonded interactions which is significant in imparting strength to the crystal structure of graphene and four body torsional interactions.AIREBO Potential is described mathematically as:

$$E^{AIREBO} = \frac{1}{2} \sum_i \sum_{j \neq i} [E_{ij}^{REBO} + E_{ij}^{LJ} + \sum_{k \neq i,j} \sum_{l \neq i,j,k} E_{kij}^{tors}] \quad (6)$$

Where i, j, k, l are different individual atoms.[18], E_{ij}^{REBO} , E_{ij}^{LJ} and E_{kij}^{tors} are the potentials of REBO,Lenard-Jones Potential which is used for Van Der Waals Forces that is used to describe interlayer interaction[19] and Interaction Potential due to torsional Potential.

RESULTS AND DISCUSSIONS

Nonequilibrium molecular dynamics simulation is carried out to study phonon properties of pristine graphene and defected graphene as phonons are associated with displacement of atoms[20].Dislocations of crystal structures are non-advantageous for the conduction of heat and is avoided in practical applications.[21] The results demonstrates that

Temporal Evolution w.r.t. time steps: Temperature is defined according to kinetic theory by taking mean kinetic energy in three directions.

$$T_i = \frac{1}{3K_B N_i} \left\langle \sum_j \left(\frac{1}{2} m_j |v_j|^2 \right) \right\rangle \quad (7)$$

Here Temperature is calculated by combining equipartition theorem with kinetic energy.[22]

To monitor temperature variation profile the temperature distribution in Kelvin with respect to timestep is plotted, here temperature curve reflect thermal states[23]In figure 3and 4 temperature distribution for pristine graphene and graphene with Stone-Wales dislocation is shown. As timesteps increases temperature is fluctuated in the range of 250K to 350K i.e. around 300K it is constant for pristine graphene and graphene with Stone-Wales dislocations as shown in figure 2.It is not affected by empirical interatomic potentials also. Temperature of each segment with respect to timestep is noted to get linear temperature gradient [22].

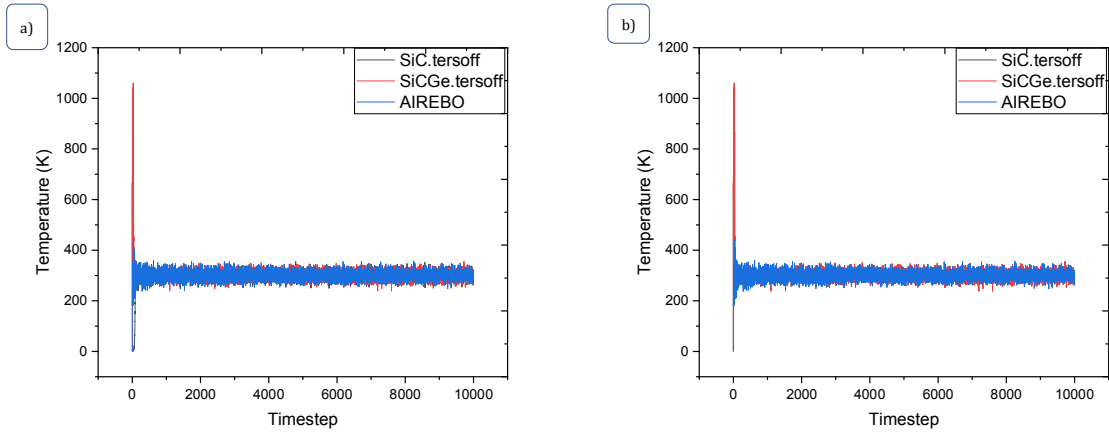


Figure 2: Time domain temperature distribution (in units of Kelvin) a) Pristine graphene b) Distorted graphene with Stone-Wales dislocation

Heat Flux (Total energy Vs Timestep):

The heat flux vector $J(t)$ is defined as

$$J(t) = \frac{d}{dt} \sum_i r_i \Delta e_i = \sum_i v_i \Delta e_i - \sum_i \sum_{j(\neq i)} r_{ij} (f_{ij} \cdot v_i) \quad (8)$$

Where e_i is energy

$$e_i = \frac{1}{2} \left(m |v_i|^2 + \sum_i \phi_{ij} \right) \quad (9)$$

For Tersoffpotential,heat flux is formulated as [22]

$$J = \frac{1}{\Omega} \left(\sum_{i=1}^n v_i e_i + \sum_{i=1}^n \sum_{j=1}^n \vec{r}_{ij} \left(\vec{v}_j \cdot \frac{\partial \phi_i}{\partial \vec{r}_j} \right) \right) \quad (10)$$

By using heat flux and temperature gradient, thermal conductivity of graphene is obtained according to Fourier's Law

$$K = -\frac{J}{\Delta T} \quad (11)$$

The figure 5 and 6 denotes the total energy in terms of electron volts with respect to time step at Tersoff and AIREBO potential for pristine graphene and graphene with Stone-wales dislocation as show. On a simulation cell, periodic boundary conditions are applied to reduce the effect of boundary scattering obtained from high frequency phonon mean free path. So resulting heat flux is written as

$$J = \frac{e}{2AdT} \quad (12)$$

Where 2 is due to heat flows from both cold and hot bin in both directions, A is area of cross section perpendicular to heat flow direction.[24]

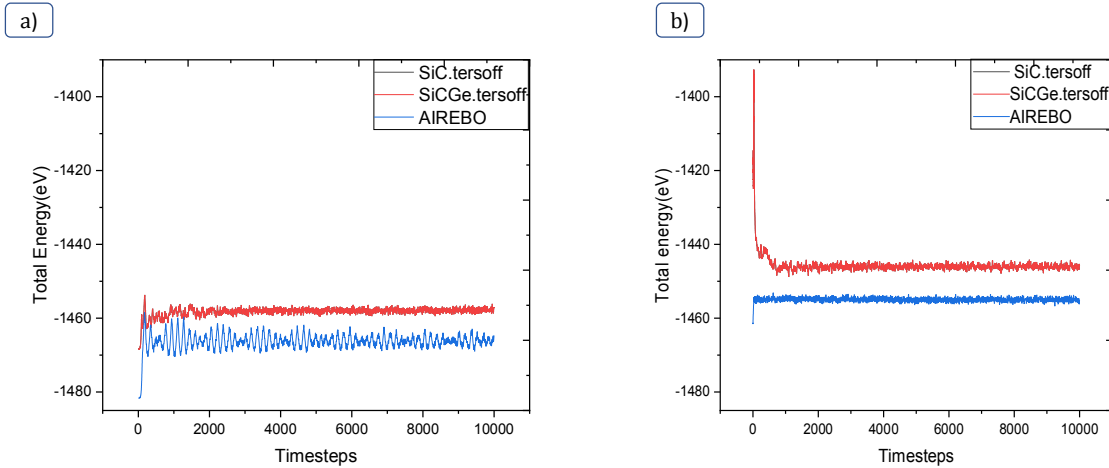


FIGURE3: Time domain total energy a) Pristine graphene at SiC.tersoff, SiCGe.tersoff Potential, AIREBO Potential b) Distorted graphene with Stone-Wales Defect at SiC.tersoff ,SiCGe.tersoff Potential, AIREBO Potential.

Phonon Density of States: G band peak is an important aspect in phonon density of states in pristine graphene. It is dependent on temperature[25].G band peak monitor's local temperature change[26]. Vibrational power spectra or phonon spectra is kinetic energy in terms of frequency ω is used to describe the state of phonons[27].

Phonon density of states make impact on properties of materials like thermal conductivity, heat capacity. Phonon density of states is computed by Fourier Transform of velocity autocorrelation function. Low frequency phonon corresponds to longer mean free path that enables phonon to propagate longer distance.

$$DOS(\omega) = \int_0^{\infty} \frac{\langle v(t)v(0) \rangle}{\langle v(0)v(0) \rangle} e^{-i\omega t} dt \quad (13)$$

Where ω is frequency and v is atomic velocity [28].The power spectrum $\hat{q}_{k,p}(t)$ [29]is calculated as

$$\Phi_{k,p}(\omega) = \left| \int \hat{q}_{k,p}(t) e^{i\omega t} dt \right|^2 \quad (14)$$

The power spectrum of phonon $P(\omega)$ is calculated from velocity autocorrelation function

$$P(\omega) = \frac{1}{\sqrt{2\pi}} \int e^{i\omega t} \left\langle \sum_{j=1}^N v_j(t)v_j(0) \right\rangle dt \quad (15)$$

Where $v_j(0)$ is velocity vector at time 0 and $v_j(t)$ is it's velocity at time t and ω is vibrational wavenumber[30].

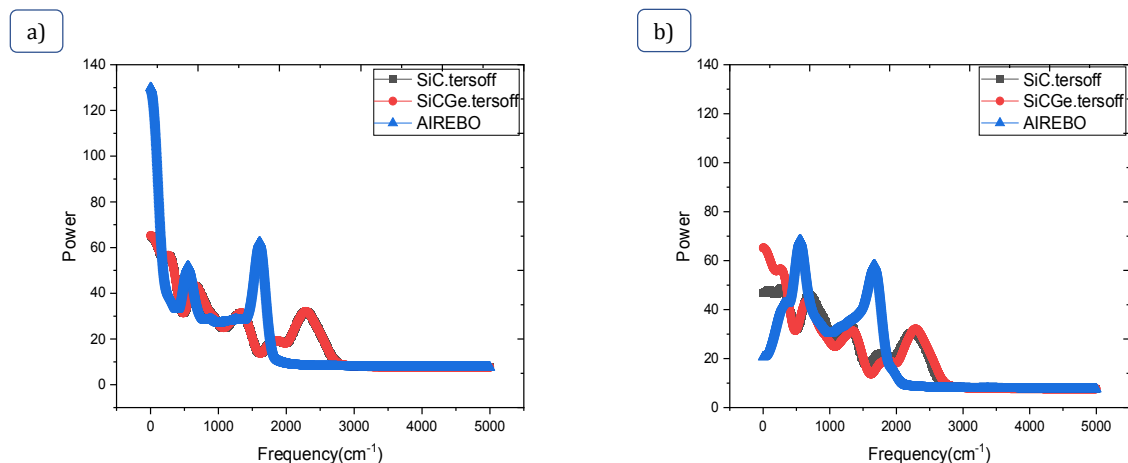


Figure 4: Phonon spectrum of a) pristine graphene with SiC.tersoff Potential, SiCGe.tersoff Potential, AIREBO Potential. b) Distorted graphene with Stone-Wales dislocations SiC.tersoff Potential, SiCGe.tersoff Potential, AIREBO Potential.

Table1: G band values of Graphene at SiC.tersoff Potential, SiCGe.tersoff Potential and AIREBO Potential

Sr.No	Frequency Domain	G peak value for SiC.tersoff Potential	G peak value for SiCGe.tersoff Potential	G peak value for AIREBO Potential
1)	Low	56.57(a.u.)	42.95(a.u.)	51.77 (a.u.)
2)	High	32.05(a.u.)	32.06 (a.u.)	62.35 (a.u.)

Frequency domain is divided into low frequency domain 0-668cm⁻¹(0-20THz),intermediate frequency domain 668-1335 cm⁻¹ (20-40 THz) and high frequency domain1335-2000cm⁻¹ (40-60 THz)domains.[24].

Table2: G band values of pristine graphene with Stone-Wales dislocation at SiC.tersoff Potential, SiCGe.tersoff Potential and AIREBO Potential

Sr.No.	Frequency Domain	G peak value for SiC.tersoff Potential	G peak value for SiCGe.tersoff Potential	G peak value for AIREBO Potential
1)	Low Frequency(0-20THz)	45.42(a.u.)	42.60(a.u.)	68.33(a.u.)
2)	High frequency(40-60THz)	30.82(a.u.)	31.66(a.u.)	58(a.u.)

As shown in Table1,the dominant peak at high frequency region of graphene for AIREBO interatomic potential reflects C-C bond interactions due to bonding. As shown in figure 4a) G band peak value 62.35(a.u.)of pristine graphene with AIREBO potential is at frequency of 1610 cm⁻¹(48.26THz) which agrees well with experimental value of Raman G band frequency 1583cm⁻¹ (47.45 THz) as given in reference[26].

The long wavelength i.e. low frequency phonons are the majority carriers of heat energy in graphene. Due to presence of dislocation, localization of majority carriers of heat shrinks heat transport capability of graphene nanosheet with Stone-Wales dislocation[31].In case of distorted graphene, phonon scattering enhances, In low frequency domain, red shift causes due to low phonon group velocities.[32] and softening of phonon modes at high frequency domain is observed which indicates reduction in thermal conductivity [31].

As seen from figure 4 b), of phonon spectrum of graphene with Stone-Wales dislocation, the peaks in the high frequency domain get softened as compared to PDOS of pristine graphene. Table 2 denotes the G band peak value is 58 (a.u) for frequency of 1671cm⁻¹(50.09THz).By comparing the Table1 and Table 2,G band peak value decreases in high frequency region. This phenomenon leads to reduction in life time and mean free path of distorted graphene with Stone-Wales dislocation. As seen from figure 4 b) in low frequency domain of distorted graphene with Stone-Wales dislocations, average increase in peaks and

broadening of peaks is observed, which reduces relaxation time and mean free path[33].The shift of phonon density of states towards low frequency shows increase in number of unsaturated C (Carbon) along with some dangling bonds in graphene with dislocations. Due to presence of Stone-Wales dislocations, thermal conductivity is reduced[17].

Radial Distribution Function: To understand the change in structural properties of pristine graphene and distorted graphene with Stone-Wales dislocation, pair correlation function is immensely required. Radial density profile (RDF) $g(r)$ of system of atoms describes that density varies with respect to distance from reference particle. It is also known as pair correlation function or pair distribution function meaning on an average how atoms in simulation cell are radially packed around each other. The number of atoms between region r and $r+dr$

$$dn(r) = \frac{N}{V} g(r) 4\pi r^2 dr \quad (16)$$

System having more than one chemical species known as partial radial distribution function[23] meaning probability density from α species to β species

$$g_{\alpha\beta}(r) = \frac{dn(\alpha\beta)r}{4\pi r^2 dr \rho_{\alpha}} \quad (17)$$

At constant temperature i.e.300K stage of NVT ensemble simulation, energy transfer is not possible and hence no thermal transport. The atomic vibrations depend only on Nose-Hoover algorithm. From RDF coordination number is defined as

$$n(r) = \int_0^r \rho_{c-c}(r) 2\pi r dr \quad (18)$$

As shown in figure 5b),In case of distorted graphene with Stone-Wales dislocation, the decrease in average area density that shortens carbon-carbon bond length As a result, distorted graphene with Stone-Wales dislocations shifts in-plane vibrational modes towards low frequency domain[24]

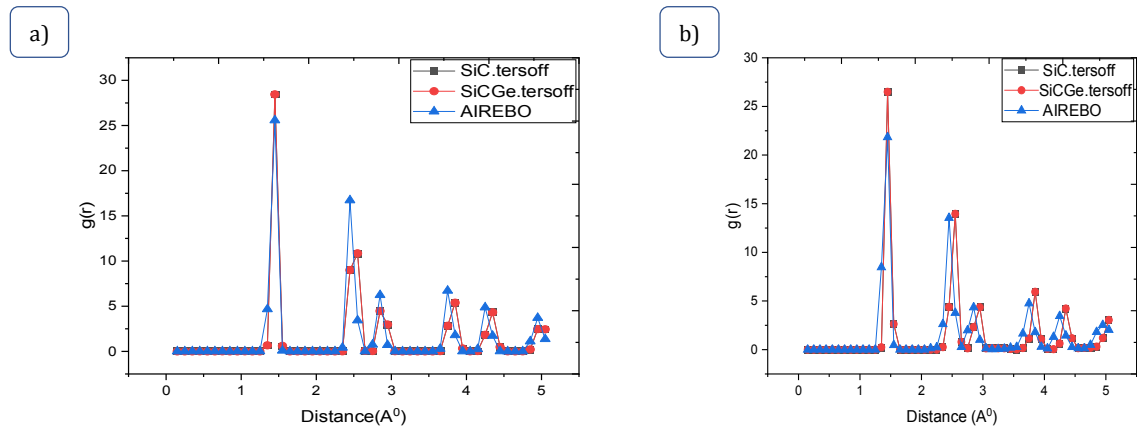


FIGURE5:Radial Distribution Function of Graphene with SiC.tersoff Potential, SiCGe.tersoff Potential, AIREBO Potential

Velocity Autocorrelation Function:

To specify dynamics of a system,velocity autocorrelation function is useful.It is time-dependent function[34]The velocity autocorrelation function is given by

$$D_i = \frac{1}{3} \int_0^{\infty} \langle \vec{V}_i(t) \cdot \vec{V}_i(0) \rangle dt = \frac{1}{3} \langle \vec{v}_i^2(0) \rangle \int_0^{\infty} z_i(t) dt \quad (19)$$

Where $\int_0^{\infty} \langle \vec{V}_i(t) \cdot \vec{V}_i(0) \rangle$ is integration of velocity autocorrelation, bracket $\langle \dots \rangle$ denotes expectation value. From Figure 6,It is seen that in case of pristine graphene, for AIREBO potential, fluctuations in VCAF within range of -0.2 to 0.2 is observed with respect to timestep. For Tersoffpotential, velocity autocorrelation function(VACF) remains decays to zero for pristine graphene and graphene with Stone-Wales dislocation.

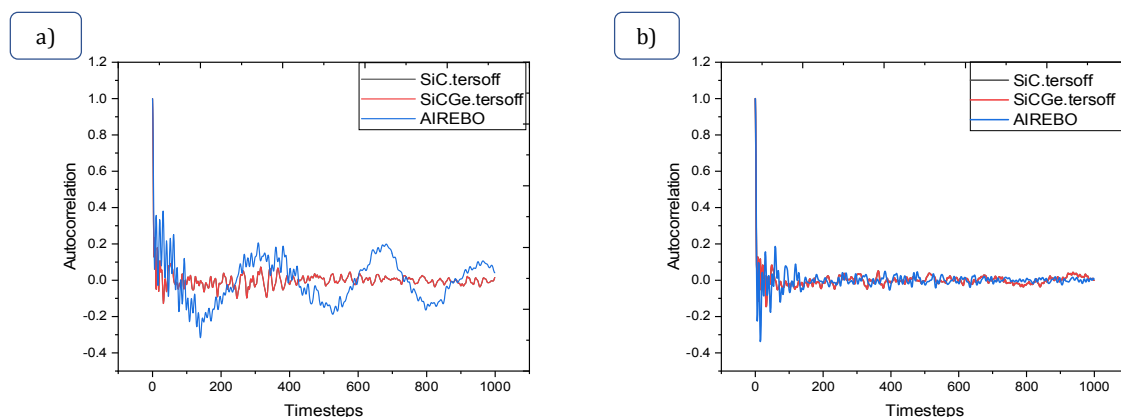


FIGURE 6: Velocity Autocorrelation Function of a) Pristine graphene for SiC.tersoff Potential, AIREBO Potential. b) Distorted graphene with Stone-Wales dislocation for SiC.tersoff Potential, AIREBO Potential

CONCLUSION

In this study, by using nonequilibrium molecular dynamics simulation method phonon spectrum of graphene and distorted graphene with Stone-Wales dislocations have been studied over interatomic potential of Tersoff Potential and AIREBO potential. The various parameters like velocity autocorrelation function (VACF) with respect to time, temperature with timesteps, potential energy with timesteps, radial density profile and phonon density of states have been studied.

In the phonon spectrum, the dominant peak at high frequency region of graphene for AIREBO interatomic potential reflects C-C bond interactions due to bonding. G band peak value 62.35(a.u.) of pristine graphene with AIREBO potential is at frequency of 1610 cm^{-1} (48.26THz) which agrees well with experimental value of Raman G band frequency 1583 cm^{-1} (47.45 THz). Due to Stone-Wales dislocations, peaks get softened at high frequency region for AIREBO potential. This result is comparable with reference[31][35]. Due to Stone-Wales dislocations the G peak (high frequency peak) [2] greatly suppressed as O:C ratio increases. As like folded graphene [36] this shows red shift towards low frequency region which slows down phonon group velocities and causes acoustic mismatch. The peaks of low frequency shows angular and dihedral diffraction within graphene (fluctuation and bending). In case of distorted graphene with Stone-Wales dislocation, the decrease in average area density as compared to pristine graphene which shortens carbon-carbon bond length.

Due to acoustic mismatch and slowing down of phonon group velocities in graphene with Stone-Wales dislocations, thermal conductivity is reduced as compared to the pristine graphene. Phonon spectrum helps to understand thermal conductivity of distorted graphene. The findings of this work are useful to reveal the phononic mechanism through defect engineering. This work is helpful to engineer low thermal conductivity nanodevices. This finding is useful to make devices in nanoelectronics.

ACKNOWLEDGEMENT

Author would like to thank Purdue University for providing computational resources.

REFERENCES

1. Zhao W, Wang Y, Wu Z, et al. (2015). Defect-Engineered Heat Transport in Graphene: A Route to High Efficient Thermal Rectification. *Sci Rep.* 5(1):1-11.
2. Zhang C, Hao XL, Wang CX, Wei N, Rabczuk T. (2017). Thermal conductivity of graphene nanoribbons under shear deformation: A molecular dynamics simulation. *Sci Rep.* 7:1-8.
3. Xu X, Pereira LFC, Wang Y, et al. (2014). Length-dependent thermal conductivity in suspended single-layer graphene. *Nat Commun.* 5:1-6.
4. Koukaras EN, Kalosakas G, Galiotis C, Papagelis K. (2015). Phonon properties of graphene derived from molecular dynamics simulations. *Sci Rep.* 5:1-9.
5. Feng T, Yao W, Wang Z, et al. (2017). Spectral analysis of nonequilibrium molecular dynamics: Spectral phonon temperature and local nonequilibrium in thin films and across interfaces. *Phys Rev B.* 95(19):195202
6. Yang X, Yu D, Cao B, To AC. (2017). Ultrahigh Thermal Rectification in Pillared Graphene Structure with Carbon Nanotube-Graphene Intramolecular Junctions. *ACS Appl Mater Interfaces.* 79(1):29-35.
7. Yang P, Li X, Yang H, Wang X, Tang Y, Yuan X. (2013). Numerical investigation on thermal conductivity and thermal rectification in graphene through nitrogen-doping engineering. *Appl Phys A Mater Sci Process.* 112(3):759-765.

8. Hong Y, Ju MG, Zhang J, Zeng XC. (2018). Phonon thermal transport in a graphene/MoSe₂ van der Waals heterobilayer. *Phys Chem Chem Phys*. 20(4):2637-2645.
9. Stukowski A. (2010). Visualization and analysis of atomistic simulation data with OVITO-the Open Visualization Tool. *Model Simul Mater Sci Eng*. 18(1):015012.
10. Rajasekaran G, Parashar A. (2016). Molecular dynamics study on the mechanical response and failure behaviour of graphene: Performance enhancement via 5-7-7-5 defects. *RSC Adv*. 6(31):26361-26373.
11. Juneja A, Rajasekaran G. (2018). Anomalous Strength Characteristics of Stone-Thrower-Wales Defects in Graphene Sheets-a Molecular Dynamics Study. *Phys Chem Chem Phys* 20(22):15202-15215.
12. Daniel Richards, Elif Ertekin, Jeffrey C Grossman, David Strubbe, Justin Riley EG. (2021). MIT Atomic-Scale Modeling Toolkit. Published online.
13. Tersoff J. Erratum: (1990). Modeling solid-state chemistry: Interatomic potentials for multicomponent systems. *Phys Rev B*. 41(5):3248.
14. Tersoff J. (1988). Empirical interatomic potential for carbon, with applications to amorphous carbon. *Phys Rev Lett*. 61(25):2879-2882.
15. Salaway RN, Zhigilei L V. (2014). Molecular dynamics simulations of thermal conductivity of carbon nanotubes: Resolving the effects of computational parameters. *Int J Heat Mass Transf*. 70:954-964.
16. Rajasekaran G, Kumar R, Parashar A. (2016). Tersoff potential with improved accuracy for simulating graphene in molecular dynamics environment. *Mater Res Express*. 63(3):035011
17. Yeo JJ, Liu Z, Ng TY. (2012). Comparing the effects of dispersed Stone-Thrower-Wales defects and double vacancies on the thermal conductivity of graphene nanoribbons. *Nanotechnology*. 23(38):385702
18. Rajasekaran G, Narayanan P, Parashar A. (2016). Effect of Point and Line Defects on Mechanical and Thermal Properties of Graphene: A Review. *Crit Rev Solid State Mater Sci*. 41(1):47-71.
19. Si C, Wang XD, Fan Z, Feng ZH, Cao BY. (2017). Impacts of potential models on calculating the thermal conductivity of graphene using non-equilibrium molecular dynamics simulations. *Int J Heat Mass Transf*. 107:450-460.
20. Yarifard M, Davoodi J, (2016). Rafii-Tabar H. In-plane thermal conductivity of graphene nanomesh: A molecular dynamics study. *Comput Mater Sci*. 111:247-251.
21. Yang D, Ma F, Sun Y, Hu T, Xu K. (2012). Influence of typical defects on thermal conductivity of graphene nanoribbons: An equilibrium molecular dynamics simulation. *Appl Surf Sci*. 258(24):9926-9931.
22. Khadem MH, Wemhoff AP. (2013). Comparison of Green-Kubo and NEMD heat flux formulations for thermal conductivity prediction using the Tersoff potential. *Comput Mater Sci*. 69:428-434.
23. Ji P, Zhang Y, Yang M. (2013). Structural, dynamic, and vibrational properties during heat transfer in Si/Ge superlattices: A Car-Parrinello molecular dynamics study. *J Appl Phys*. 114(23).
24. Verma A, Kumar R, Parashar A. (2019). Enhanced thermal transport across a bi-crystalline graphene-polymer interface: An atomistic approach. *Phys Chem Chem Phys*. 21(11):6229-6237.
25. Zou JH, Ye ZQ, Cao BY. (Phonon thermal properties of graphene from molecular dynamics using different potentials. *J Chem Phys*. 2016;145(13):134705
26. Balandin AA, Ghosh S, Bao W, et al. Superior thermal conductivity of single-layer graphene. *Nano Lett*. 2008;8(3):902-907.
27. Zhu F, Kan Y, Tang K, Liu S. Investigation of Thermal Properties of Ni-Coated Graphene Nanoribbons Based on Molecular Dynamics Methods. *J Electron Mater*. 2017;46(8):4733-4739.
28. Mortazavi B, Fan Z, Pereira LFC, Harju A, Rabczuk T. (2016). Amorphized graphene: A stiff material with low thermal conductivity. *Carbon N Y*. 103:318-326.
29. Hu S, Chen J, Yang N, Li B. (2017). Thermal transport in graphene with defect and doping: Phonon modes analysis. *Carbon N Y*. 16:139-144.
30. Liang Q, Wei Y. (2014). Molecular dynamics study on the thermal conductivity and thermal rectification in graphene with geometric variations of doped boron. *Phys B Condens Matter*. 437:36-40.
31. Noshin M, Khan AI, Navid IA, Uddin HMA, Subrina S. (2017). Impact of vacancies on the thermal conductivity of graphene nanoribbons: A molecular dynamics simulation study. *AIP Adv*. 7(1):015112
32. Cui L, Du X, Wei G, Feng Y. (2016). Thermal Conductivity of Graphene Wrinkles: A Molecular Dynamics Simulation. *J Phys Chem C*. 120(41):23807-23812.
33. Zhang H, Lee G, Cho K. (2018). Thermal transport in graphene and effects of vacancy defects. *Phys Rev B - Condens Matter Mater Phys*. 84(11):1-5.
34. See TL, Feng RX, Lee CY, Stachurski ZH. (2012). Phonon thermal conductivity of a nanowire with amorphous structure. *Comput Mater Sci*. 59:152-157.
35. Hao F, Fang D, Xu Z. (2011). Mechanical and thermal transport properties of graphene with defects. *Appl Phys Lett*. 99(4):1-3.
36. Zhang Z, Xie Y, Peng Q, Chen Y. (2015). Geometry, stability and thermal transport of hydrogenated graphene nanoquills. *Solid State Commun*. 213-214:31-36.

CITATION OF THIS ARTICLE

P. P. Jadhav, and R.S. Vhatkar. Phonon Spectrum of Distorted Graphene with Stone-Wales Dislocations at Tersoff and Airebo Potential. *Bull. Env. Pharmacol. Life Sci., Spl Issue* [1] 2022 : 1476-1483